Mechanical Strength of Humidified Glass Beads

C. SoriaHoyo, J. M. Valverde, and A. Castellanos

Citation: AIP Conference Proceedings **1145**, 903 (2009); doi: 10.1063/1.3180076
View online: http://dx.doi.org/10.1063/1.3180076
View Table of Contents: http://scitation.aip.org/content/aip/proceeding/aipcp/1145?ver=pdfcov
Published by the AIP Publishing

Articles you may be interested in

Hybrid grid and tree structures for cooling and mechanical strength
J. Appl. Phys. **110**, 064910 (2011); 10.1063/1.3626062

Vascular structures for volumetric cooling and mechanical strength
J. Appl. Phys. **107**, 044901 (2010); 10.1063/1.3294697

Fractal network dimension determining the relation between the strength of bulk metallic glasses and the glass transition temperature
Appl. Phys. Lett. **95**, 021909 (2009); 10.1063/1.3183520

Indentation depth dependence of the mechanical strength of Ni films
J. Appl. Phys. **103**, 043512 (2008); 10.1063/1.2885090

Unified equation for the strength of bulk metallic glasses
Appl. Phys. Lett. **88**, 221911 (2006); 10.1063/1.2206099

This article is copyrighted as indicated in the article. Reuse of AIP content is subject to the terms at: http://scitation.aip.org/termsconditions. Downloaded to IP: 150.214.138.224 On: Fri, 23 Jan 2015 09:02:05

Mechanical Strength of Humidified Glass Beads

C. Soria-Hoyo, J. M. Valverde and A. Castellanos

Faculty of Physics. University of Seville. Avenida Reina Mercedes s/n, 41012 Seville. Spain.

Abstract. In this work we measure the mechanical strength of a bed of glass beads that has been previously subjected to a controlled flow of humid air by using a fluidized bed setup. The material is first initialized in a reproducible state by subjecting it to a high flow of dry air that drives the bed to bubbling. Then the gas flow is abruptly turned off and, once the bed is settled, it is subjected to a small flow of humid air during a certain period of time. Water moisture is added to the fluidizing air by bubbling it through water. The relative humidity and dew point of the air are monitored on-line by using humidity sensors upstream and downstream of the bed. After the stationary condition is reached, the bed is slowly tilted and the avalanche angle and depth are measured. From Coulomb's wedge model and Rumpf's equation using the attractive capillary force, the predicted angle of avalanche of the humidified samples is shown to be close to the experimental value.

Keywords: Cohesion, Humidity, Avalanches
PACS: 45.70.-n, 45.70.Ht, 92.60.jk

A common characteristic of avalanches in dry granular media is that granular motion does occur in a relatively thin boundary layer (around 10 grains) at the surface independently of the size of the sample [1]. The reason for this behavior is the lack of cohesion between grains. Several studies are dedicated to understand the effect of cohesion induced by moisture in the angle of repose of the material [2]. A familiar example of moisture induced cohesion is wet sand. Typical diameters of sand particles range from 100 to 500 μm. Inter-particle capillary forces in wet sand due to liquid bridges can exceed particle weight in two to three orders of magnitude [3]. As a consequence cohesive effects are dominant in its bulk behavior. It is well known that, as opposed to dry sand, wet sand yields in internal slip surfaces, macroscopic blocks of wet sand detach from the bulk, and sample size is determinant in the slope stability.

In the continuum approach, the onset of flow is characterized by an empirical limiting stress function, the yield locus, such that stresses lower than this limit cause negligible deformation, whereas at this limit there will be a combination of shear and compression stresses that will trigger the avalanche. At high stresses the yield locus can be approximated by a linear function known as Coulomb's law [4]

$$\tau = \sigma \tan\phi + c \tag{1}$$

where τ and σ are the tangential and normal stresses over the slip plane (i.e. the plane over which the yield condition is satisfied), c and ϕ are called the cohesion and the angle of internal friction. The point of the yield locus on the negative σ-axis is called tensile strength $\sigma_t = c/\tan\phi$, which is the maximum tensile stress that the powder can withstand.

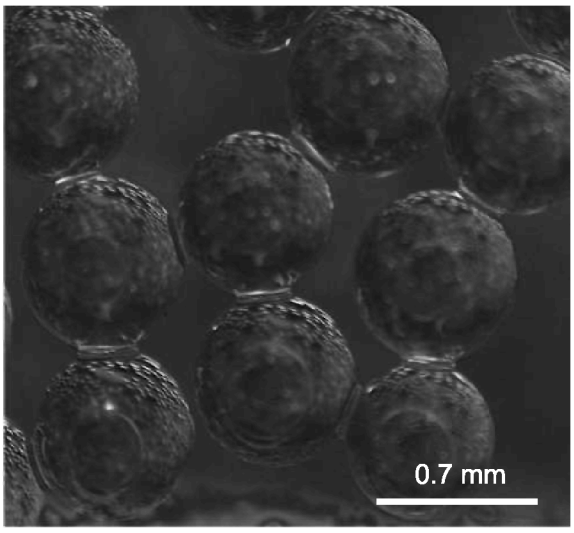

FIGURE 1. Optical microscope photograph of humidified granular beads

The tensile strength of a granular material is caused by interparticle cohesive forces. When a granular material is in contact with moist air, water vapor is appreciably adsorbed on the surface of the grains and, if humidity approaches saturation, capillary condensation occurs and liquid bridges form at the contact between the grains as can be seen in Fig. 1. In the pendular state, in which liquid saturation causes the formation of liquid bridges between the grains particles, the tensile strength of randomly packed, monosized grains can be estimated as [3]

$$\sigma_t \simeq \frac{1-\varepsilon}{\varepsilon}\frac{F_t}{d_p^2} \tag{2}$$

CP1145, *Powders and Grains 2009, Proceedings of the 6th International Conference on Micromechanics of Granular Media* edited by M. Nakagawa and S. Luding
© 2009 American Institute of Physics 978-0-7354-0682-7/09/$25.00

This article is copyrighted as indicated in the article. Reuse of AIP content is subject to the terms at: http://scitation.aip.org/termsconditions. Downloaded to IP: 150.214.138.224 On: Fri, 23 Jan 2015 09:02:05

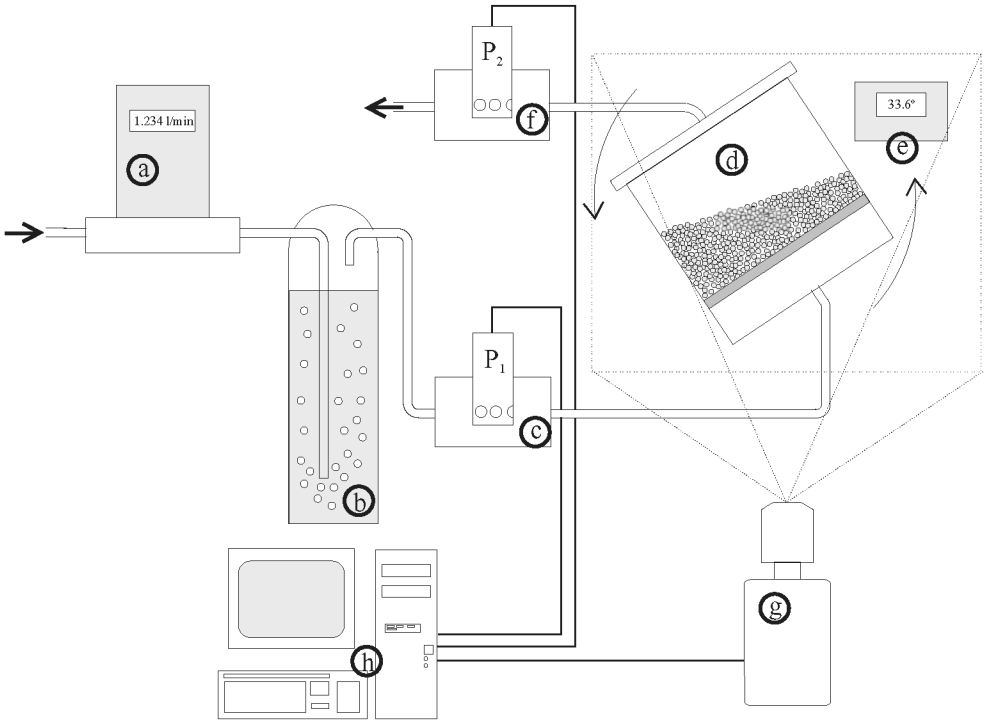

FIGURE 2. Sketch of the experimental setup used in the experiments; a: mass flow controller; b: air bubbling flask; c: temperature and humidity probe; d: granular material cell; e: inclinometer; f: temperature and humidity probe; g: video camera connected to a computer (h) for image processing.

where ε is the bed porosity, d_p is grain size, and F_t is the interparticle attractive force. In the case of dry granular materials, the dominant interaction is the van der Waals interaction, which gives $F_t \simeq 10$ nN [5]. For humidified granular materials, this force can be greatly enhanced. The capillary force between two equal spheres of radius $r = d_p/2$ can be approximated by $F_t \simeq \pi\gamma r^2\beta/S$, where γ is the liquid surface tension, β is the half-filling angle and S is the separation distance [6]. In the limit in which the volume of liquid is negligible as compared to the volume of solids and the separation distance between the particles is much smaller than their size, we can write $F_t \simeq \pi\gamma d_p/2$ [7]. Thus,

$$\sigma_t \simeq \frac{1-\varepsilon}{\varepsilon}\frac{\pi}{2}\frac{\gamma}{d_p} \tag{3}$$

In the range of bead sizes tested in our experiment (0.4 mm$< d_p <$ 4 mm), the tensile strength of the dry beads is fully negligible. On the other hand, moistening increases the tensile strength by several orders of magnitude and, as we will see, this induced cohesiveness has a relevant effect on the avalanche angle of the moistened beads.

In our experiments we have tested the cohesion of humidified samples of of soda-lime glass beads of several diameters, ranging from d_p=0.4 mm to d_p =4 mm, and particle density $\rho_p \simeq 2500$ kg/m^3. The setup used in the experiments is schematized in figure 2. The mass flow controller (labeled as *a* in figure 2) supplies a controlled gas flow (1000 cm^3/min) of filtered and dried air to the entrance of a flask (*b*), where the air is bubbled continuously through water at ambient pressure and temperature ($\gamma = 72.75$ mN/m) to moisten it up to 100% relative humidity (RH). The humidified air flow passes through a cell (*c*), where a humidity and temperature probe (P_1) monitors it continuously. The granular sample is contained in a methacrylate cell (*d*, 20×4 cm^2 cross section), with a horizontal porous plate of sintered steel at its bottom (in grey in figure 2) on which the granular bed rests. The relativity humidity of the air abandoning the cell is measured by another probe (P_2) at cell (*f*) before being exhausted out. The cell is humidified in two steps. First, humid air flows through the empty cell for several hours, until the relative humidity monitored by the two probes P_1 and P_2 are labeled to 100% RH. Once a uniform humid state of the cell is reached the dry granular sample is introduced in the cell and the flow of humid air is kept on until the reading of probes P_1 and P_2 are labeled again to 100% RH. Once the granular bed is humidified, the cell is slowly tilted at an angular speed of 8^0 per minute, increasing the angle from zero until the humidified granular bed avalanches. To eliminate vibrations in the tilt drive we installed a multiple gear train, driven by

This article is copyrighted as indicated in the article. Reuse of AIP content is subject to the terms at: http://scitation.aip.org/termsconditions. Downloaded to IP: 150.214.138.224 On: Fri, 23 Jan 2015 09:02:05

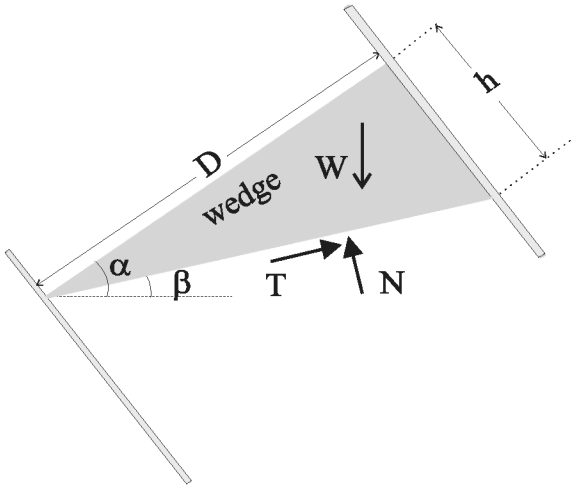

FIGURE 3. Triangular wedge model. The fracture surface is assumed to be a plane inclined at an angle $\beta < \alpha$. Normal and tangential stresses acting on the slip surface are represented.

a d.c. electric motor. As the angle of tilt increases, a shear stress is generated in the humidified granular layer. There comes a point at which the sample fails in shear and a layer of grains slumps to one side of the bed. The tilting process is video recorded at a rate of 25 frames per second. The camera was connected to a computer for image processing and the tilt angle (measured by an inclinometer (e)) at which the humidified granular bed avalanches (α) is measured as a function of bed width. The problem then is to relate the angle of avalanche to the cohesion of the humidified granular bed.

The theoretical analysis of the slip problem is based on Coulomb's method of wedges [4]. The underlying assumptions in the method of wedges are: (i) that failure occurs along a slip surface which is planar, (ii) that the stresses at the slip surface are related to the values specified by the yield condition (Mohr-Coulomb yield locus [4]), and (iii) that the condition of critical equilibrium holds (i.e. just before the avalanche we can assume a balance of forces in the sliding wedge). The method is commonly applicable to two-dimensional situations, such as the calculation of the force on an infinite retaining wall [4]. One of the standard applications of the method of wedges [4] is the analysis by geologists of hill slope, as when topographically induced gravitational shear stress exceeds the strength of the material and a landslide occurs. The geometric arrangement of Fig. 3 shows a hypothetical slip plane. From Fig. 3 wedge equilibrium equations

$$T\cos\beta - N\sin\beta = 0, \quad (4)$$

$$T\sin\beta + N\cos\beta = W, \quad (5)$$

and yield condition

$$T = N\tan\phi + c\frac{D}{\cos(\alpha-\beta)} \quad (6)$$

follow, where T and N are the tangential and normal forces respectively over the slip plane, $W = 1/2\rho_p(1-\varepsilon)gD^2\tan(\alpha-\beta)$ is the wedge weight, where g=9.81 m/s^2 is gravity acceleration, $\varepsilon \simeq 0.5$ is the bed porosity, and $D/\cos(\alpha-\beta)$ is the length of the slip plane. Equations 4, 5 and 6 must be satisfied with two unknowns, T and N. A slip plane appears when the set of three equations is compatible. The condition for compatibility gives a functional relation $\alpha = \alpha(\beta)$ between the angle of tilt α, and the angle β. The function $\alpha(\beta)$ has an absolute minimum α_{min} at a given value of β_0. Now, if we slowly tilt the bed, a slip plane is not formed until the angle α_{min} is reached. Once this angle is reached the powder avalanches, and the value of β_0 determines the avalanche depth. Operating, we obtain

$$\beta_0 = \frac{\alpha+\phi}{2} \quad (7)$$

$$\rho_p(1-\varepsilon)gD = 4c\cos\phi\,(1-\cos(\alpha-\phi))^{-1}. \quad (8)$$

From equation 8 it is apparent the key role played by powder cohesion c and bed width D on the onset of avalanches. In the noncohesive limit, $c/(\rho_p gD) \to 0$, $\alpha \to \phi$ as expected.

Data measured for the angle of avalanche are shown in Fig. 5 for both dry and moistened beds. It is observed that for the dry beds the angle of avalanche is almost independent of the bead size. This result can be rationalized on the basis that the ratio $\sigma_t/(\rho_p(1-\varepsilon)gD)$ calculated for these dry beads is negligible. Thus, according to Eq. 8, the angle of avalanche should be very close to the angle of internal friction ($\alpha \simeq \phi$), which is seen not to depend essentially on bead size in the range of sizes tested. Indeed, the values measured are around 26^0, which is about the angle of internal friction measured for fine glass beads using a Ring Shear Tester and a Centrifuge Tester (see [8] for additional details on this measurements). In contrast, it is observed in Fig. 5 that the angle of avalanche for the moistened beds is larger than the angle of internal friction as should be expected because of the induced cohesiveness. It must be noted also that the shape of avalanches is radically changed by moistening. While for the dry samples the avalanche involves a thin superficial layer of grains, for the moistened samples the yield occurs deep inside the bed as can be seen in Fig. 4. Using the avalanche angle data of the dry beds to estimate the angle of internal friction ($\alpha \simeq \phi$) and using the calculated tensile strength σ_t (Eq. 3), we may obtain from Eq. 8 the avalanche angle predicted by the continuum model for the moistened beds. The predicted

This article is copyrighted as indicated in the article. Reuse of AIP content is subject to the terms at: http://scitation.aip.org/termsconditions. Downloaded to IP: 150.214.138.224 On: Fri, 23 Jan 2015 09:02:05

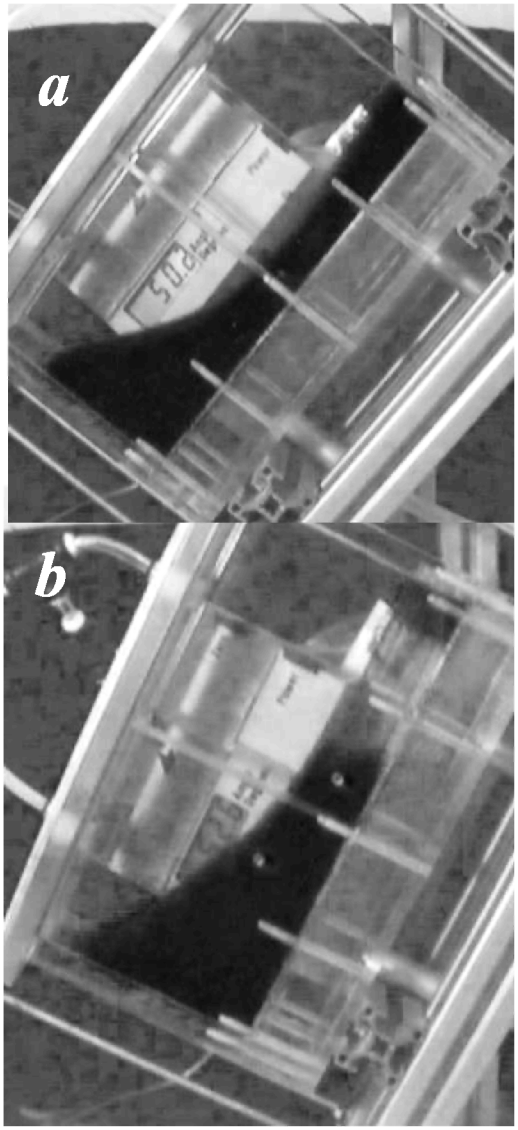

FIGURE 4. Snapshot of the tilted granular bed after the avalanche. a: Moistened 1-1.25 mm sized beads; b: Moistened 0.40-0.60 mm sized beads.

data in this way are plotted in Fig. 5, where it can be observed that, in spite of the simplicity of the model, the predicted data are close to the experimental values. This result suggests that Eq. 8 can be used as a simple analytical tool to obtain a good estimation of the avalanche angle of cohesive granular materials. Moreover, the results indicate that Eq. 3 is a also good estimation for the tensile strength of moistened granular beds in the pendular state.

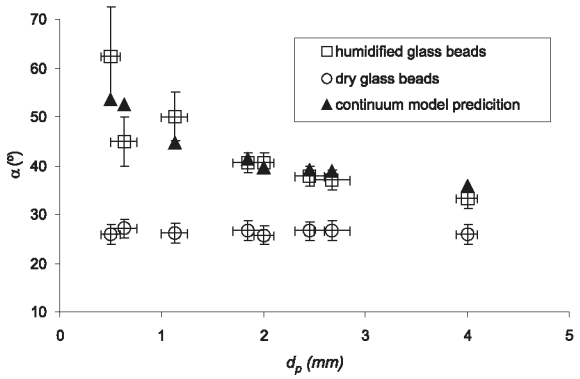

FIGURE 5. Angle of avalanche of moistened and dry beds as a function of bead size. The model predictions for moistened beds are also plotted.

ACKNOWLEDGMENTS

We acknowledge Spanish Government Agency Ministerio de Ciencia y Tecnologia (contract FIS2006-03645) and Junta de Andalucia (contract FQM 421).

REFERENCES

1. H. M. Jaeger and S. R. Nagel, Science **255**, 1523 (1992).
2. L. Bocquet, E. Charlaix, S. Ciliberto and J. Crassous, Nature **396**, 735 (1998).
3. H. Schubert, Powder Technol. **37**, 105 (1984).
4. R. Nedderman. *Statics and Kinematics of Granular Materials* (Cambridge University Press, UK 1992).
5. A. Castellanos, Adv. Phys. **54**, 263 (2005).
6. C.D. Willett, M.J. Adams, S.A. Johnson, and J.P.K. Seville. Langmuir **16**, 9396 (2000).
7. P. Pierrat, H. S. Caram, Powder Technol. **91**, 83-93 (1997).
8. C. Soria-Hoyo, J.M. Valverde, A. Castellanos, AIChE J. **54**, 886 (2008).

This article is copyrighted as indicated in the article. Reuse of AIP content is subject to the terms at: http://scitation.aip.org/termsconditions. Downloaded to IP: 150.214.138.224 On: Fri, 23 Jan 2015 09:02:05